

Indenofluorenes

π -Extended Indenofluorenes

M. Rajeswara Rao, Antonin Desmecht, and Dmitrii F. Perepichka*^[a]

Abstract: A series of π -extended aromatic indenofluorene (IF) analogues with naphthalene and anthracene cores have been synthesized through acid-catalyzed intramolecular cyclization. The regioselectivity of the reaction is controlled by a combination of steric and electronic factors and in some cases several possible regioisomers have resulted from the same precursor. The effects of ring connectivity on the optoelectronic properties were investigated by DFT calculations,

absorption/emission spectroscopy, cyclic voltammetry, and spectroelectrochemical studies. All regioisomers exhibited a redshift of their absorption/emission bands relative to the parent IF analogues, but the magnitude of this shift and other optoelectronic properties (luminescence quantum yield, etc.) depends on the ring connectivity in a less obvious manner.

Introduction

For the past two decades the interest in structure–property relationships in π -conjugated systems has been fueled by their applications in various optoelectronic devices.^[1] Fluorene, a rigid planar aromatic hydrocarbon, and its numerous derivatives^[2] have gained a lot of attention in optoelectronics due to their high stability, efficient light emission, and reasonable charge-transport properties. Polyfluorenes are considered bread-and-butter materials for blue organic light-emitting diodes (OLEDs)^[3] and solid-state lasers.^[4] Also, fluorene-based copolymers have found numerous applications in thin-film transistors^[5] and solar cells.^[6]

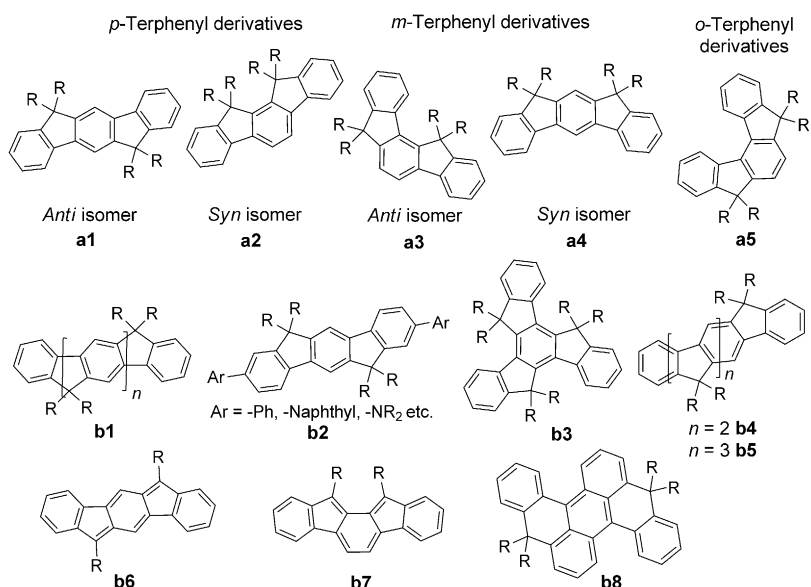
The electronic and optical properties of fluorene principally arise from its rigidity where an sp^3 bridge carbon atom “locks” the two benzene rings in a planar structure. However, free rotation around a C–C bond between fluorene units in corresponding polymers leads to a relatively flexible structure (with possible nonplanar conformations). To extend an oligo/polyphenylene π -electron structure without compromising the rigidity of the formed material, sp^3 bridge atoms should be introduced between each neighboring aromatic ring, as exemplified by indenofluorene (IF) **a1** or ladder poly(*p*-phenylene) (LPPP; **b1**).^[7] An efficient π conjugation in a fully coplanar LPPP backbone leads to a number of interesting properties including increased photoluminescence efficiency^[8] and charge mobility.^[9] The dihydroindenofluorene core (**a1**) was shown to be a promising building block for conjugated polymers for

a broad variety of applications, in blue OLEDs,^[10] organic field-effect transistors,^[11] and organic solar cells.^[12] Varying the connectivity of the benzene rings in IF isomers **a1–a5** allows for tuning of their bandgap and triplet energy, thus affording highly efficient electroluminescent molecular materials and high triplet energy hosts for phosphorescent OLEDs.^[13,14]

A number of other structurally modified IFs have been exploited^[15–17] with the goal of tailoring the electronic and optical characteristics of thin-film devices. The π conjugation of the IF core was further extended to the peripheral substituents (**b2**)^[15] and by annulation of terminal benzene rings.^[18] Truxene **b3**, a C_3 -symmetric analogue of IF, has become a highly popular core for star-shaped conjugated oligomers, with myriad applications.^[19–21] Linearly extended fully fused IFs **b4** and **b5** have also been studied, as well-defined molecular analogues of LPPP **b1**.^[16] Despite the apparent variety of the IF-type structures, their properties are not dramatically different, which can be explained by large aromatic stabilization of their benzene ring constituents, and thus limited π -electron delocalization in the ground state. For example, most of the emission of IFs **a1–a5** falls in the UV range of the spectrum. This “electron confinement” effect can be alleviated by replacing the sp^3 -hybridized bridge of dihydroindenofluorene with an sp^2 carbon atom, as was demonstrated for compounds **b6**^[22] and **b7**.^[23] The quinoidalization of the central benzene ring and formally antiaromatic character renders these molecules very different electronic properties, including dramatically lowered HOMO–LUMO gap and ambipolar charge transport. Less is known about the structural effects of other aromatic rings in the IF motif,^[16a,18,24,25] although such extension of the π -electron system would allow widening of the range of optoelectronic properties while maintaining all the advantages of the rigid IF-type structure. Of close relevance to the present paper, several analogues of LPPP polymer with a naphthalene moiety in the main chain have been described.^[25b] Also, the diphenylanthracene derivative **b8** with planarizing sp^3 bridges was reported.^[25a]

[a] Dr. M. R. Rao, A. Desmecht, Prof. D. F. Perepichka
Department of Chemistry and Centre for Self-Assembled
Chemical Structures
McGill University
Montreal, QC H3A 0B8 (Canada)
E-mail: dmitrii.perepichka@mcgill.ca

 Supporting information for this article is available on the WWW under
<http://dx.doi.org/10.1002/chem.201406646>.



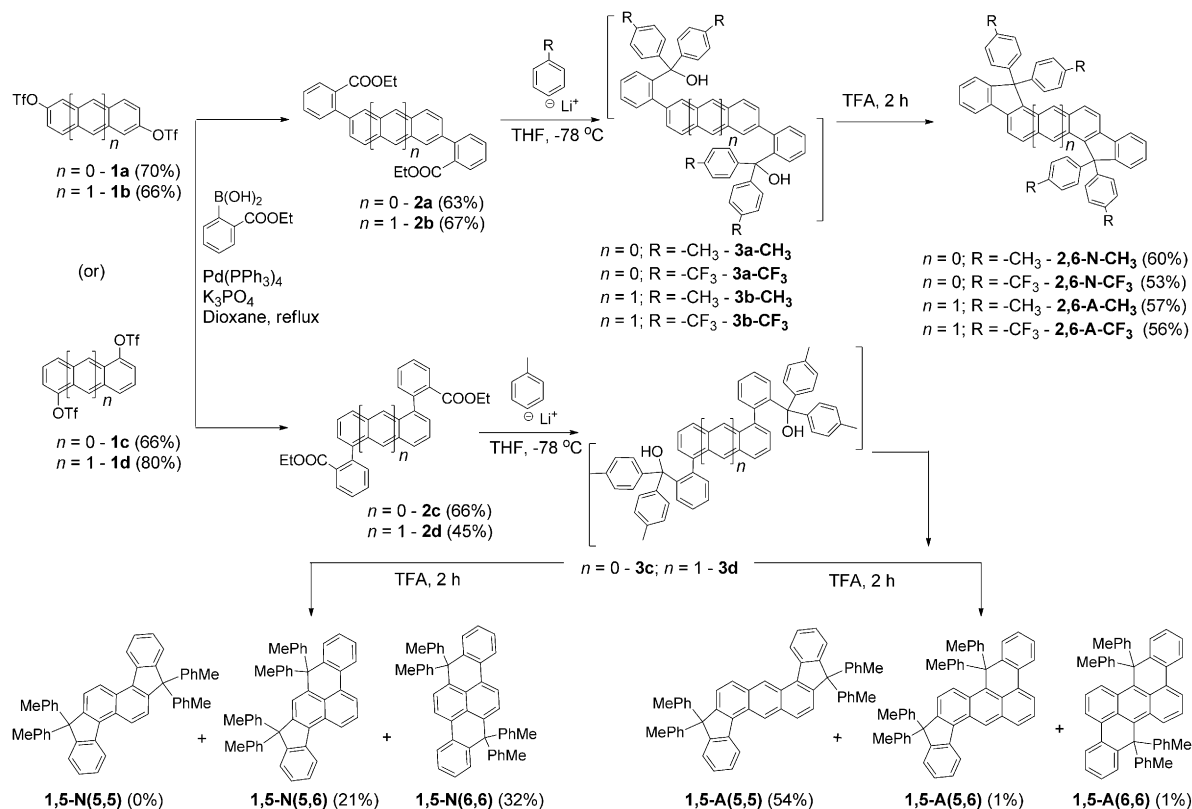
Herein, we report a series of new molecular IF analogues based on naphthalene (BINs) and anthracene (BIAs) cores, with various connectivities. Different regiosomers were achieved through an expedient synthesis utilizing double electrophilic cyclization of the substituted acene precursors. The optical, electrochemical, and structural properties of the BIN/BIA compounds were explored and compared with those of IF homologues to understand the effect of π -electron topology on

the optoelectronic properties of these polycyclic aromatic hydrocarbons.

Results and Discussion

Synthesis

We identified naphthalene/anthracene triflates **1a-d** as the key intermediates that provide access to the entire series of designed isomers (Scheme 1). The former were obtained in good yields (65–80%) by reaction of the corresponding diols with triflic anhydride, in the presence of triethylamine. The precursor naphthalenediols were commercially available whereas anthracenediols were synthesized from the corresponding dihydroxyanthraquinones (see the Supporting Information). Suzuki–Miyaura coupling of the triflates **1a-d** with 2-(ethoxycarbonyl)phenylboronic acid gave intermediates **2a-d** in 45–65% yields. The diesters **2a-d** were subjected to nucleophilic addition of *p*-tolyllithium or *p*-trifluoromethylphenyllithium, thereby affording the tertiary alcohols **3a-d**. Subsequent acid-catalyzed intramolecular cyclization of **3a-d** in neat trifluoroacetic acid (TFA)



Scheme 1. Synthesis of 2,6-/1,5-naphthalene and anthracene indenofluorenes (BINs and BIAs). OTf = triflate.

at room temperature afforded the target BINs and BIAs. Screening of reaction temperatures, catalyst (HCl, TFA, and $\text{BF}_3\cdot\text{Et}_2\text{O}$), and concentration did not show a significant effect either on the yield or the isomeric ratios. Statistically, the cyclization on each side might occur through one of the two carbon atoms of the acene unit neighboring the carbinol substituent, to yield three possible regioisomers. In contrast to the previously reported synthesis of isomeric (not π -extended) IFs,^[15–17] intramolecular cyclization of 2,6-disubstituted diols **3a** and **3b** led to almost exclusive formation of 1,5-cyclized symmetric isomers (**2,6-N** and **2,6-A**), confirmed by ^1H NMR spectra of reaction mixtures. This could be attributed to the known higher nucleophilicity of *peri* positions of naphthalene/anthracene rings.^[26] In contrast, the intramolecular cyclization of 1,5-diols **3c** and **3d** led to the formation of several regioisomers. Interestingly, naphthalene and anthracene diols showed a different regiocontrol. Although symmetric products have prevailed in both reactions, naphthalene derivative **3c** preferred to form six-membered cycles, thus yielding two isomers **1,5-N(6,6)** and **1,5-N(5,6)** in 60:40 ratio. In contrast, its anthracene congener **3d** produced **1,5-A(5,5)**, **1,5-A(6,6)**, and **1,5-A(5,6)** in 95:3:2 ratio.^[27] Symmetric (5,5)/(6,6) isomers are less soluble than asymmetric (5,6) isomers, which allowed pure isomers to be obtained by recrystallization. The combined yields of both isolated isomers are in each case above 50%. Their structures were ascertained by a combination of ^1H NMR spectroscopy and X-ray crystallography (see below).

The different isomeric ratios observed for naphthalene and anthracene can be rationalized by two factors: 1) higher nucleophilicity of the aromatic carbon atoms in the *peri* position (which favors formation of 6,6-isomers) and 2) relative steric strain of the isomers (which favors formation of less hindered 5,5-isomers). Density functional theory (DFT) calculations showed that **1,5-N(6,6)** is destabilized with respect to **1,5-N(5,6)** and **1,5-N(5,5)** isomers by 0.8 and 1.6 kcal mol⁻¹, respectively, as a result of mild steric strain. A competition between this steric strain (of the corresponding transition state), which should be smaller for cyclization through five-membered rings, and higher nucleophilicity of the *peri* positions in the naphthalene (that favors cyclization through six-membered rings) explains why both (5,6) and (6,6) isomers are formed in similar quantities (40:60). In the anthracene series, the steric strain is much more pronounced: **1,5-A(6,6)** is thermodynamically less stable than **1,5-A(5,6)** and **1,5-A(5,5)** isomers by 11.3 and 21.6 kcal mol⁻¹, respectively (see the Supporting Information). Such large destabilization of the (6,6) and (5,6) isomers, which should also be reflected in the corresponding transition states, overshadows the difference in nucleophilicity and explains the almost exclusive formation of the (5,5) isomer. A relevant interplay of electronic and steric factors on the isomeric ratio of IFs **a1/a2** through a similar electrophilic cyclization reaction has been recently investigated in detail.^[28]

All synthesized compounds are readily soluble in common organic solvents (CHCl_3 , THF, ether, etc.) except **1,5-A(5,5)**, which was only soluble in hot chlorinated solvents (e.g., tetrachloroethane or trichlorobenzene).

X-ray crystal structure analysis

Single crystals of **1,5-N(6,6)** and **1,5-A(5,5)** were grown by physical vapor transport at approximately 150 °C and ambient pressure, in a flow of argon, whereas slow evaporation of chloroform solution was employed for **2,6-A-CH₃**. In the latter case, the prolonged exposure to air and light (over 3 months) led to the unexpected formation of the endoperoxide of **2,6-A-CH₃**, which nevertheless proved the regiochemistry of this isomer (Figure 1 e,f). All three crystals are triclinic with the

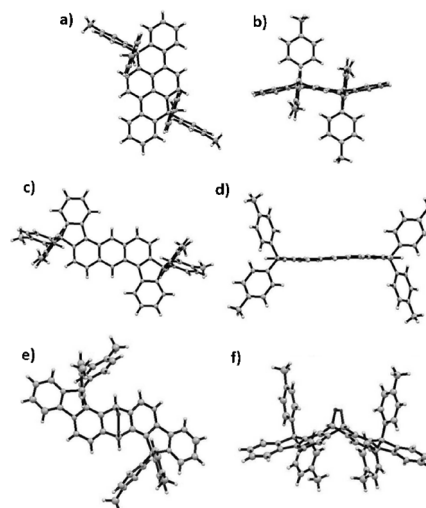


Figure 1. Crystal structures of **1,5-N(6,6)** (a, b), **1,5-A(5,5)** (c, d), and **2,6-A-CH₃** endoperoxide (e, f); (a), (c), and (e): top view and (b), (d), and (f): side view.

space group $P\bar{1}$. In **1,5-A(5,5)** the π -conjugated core is nearly planar (dihedral angle between the anthracene and terminal benzene rings of 4.4°; Figure 1 c,d) whereas a substantial “saddle-shaped” twist was noticed in **1,5-N(6,6)** (19.8°; Figure 1 a,b). This can be attributed to steric clashes between the tolyl substituents and *peri* hydrogen atoms of the naphthalene core, and the relative flexibility of six-membered rings, which allow minimization of the steric repulsions by distortion.

In the crystal of **1,5-A(5,5)**, the molecules are arranged in one-dimensional slipped stacks with a very limited π overlap (of three carbon atoms) of the terminal benzene rings and interplanar distance of 3.74 Å. In addition, there are a few weak C–H…π contacts between tolyl substituents of adjacent **1,5-A(5,5)** molecules with an interaction distance of approximately 3.2 Å. Similarly, **1,5-N(6,6)** also showed no π stacks in the crystal packing with only weak π – π interactions taking place through C–H…π contacts (\approx 3.2 Å).

Electronic structure calculations

The calculated (B3LYP/6-31G(d)) gas-phase structures resemble closely those found in the solid state by X-ray analysis. The conjugated backbone in all (5,5) isomers is almost planar (\approx 2–5°) whereas (5,6) and (6,6) isomers possess significant twist distortion (12–22° and 19–30°, respectively). The calculated bond

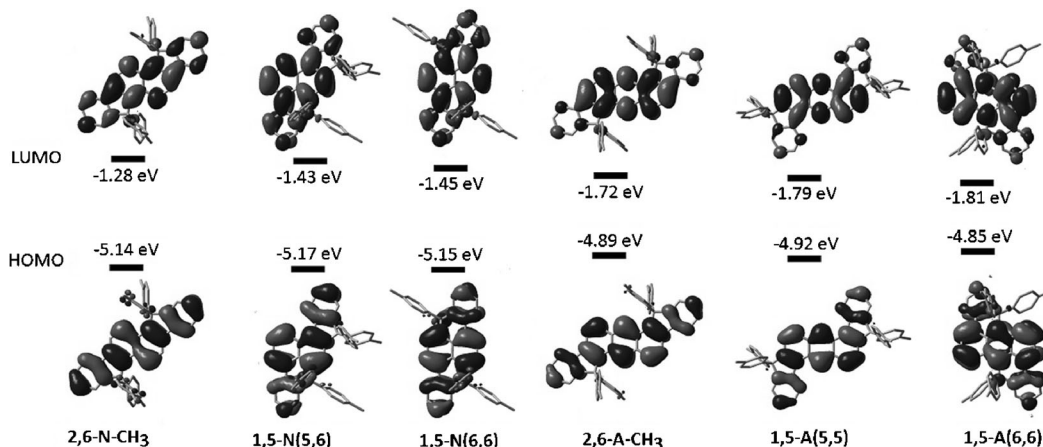


Figure 2. DFT (B3LYP/6-31G(d)) calculated frontier molecular orbital energies and surface topologies of BINs and BIAs.

lengths in the central IF core match the experimentally observed values within 0.01 Å, thus reaffirming the accuracy of the chosen theoretical level for these molecular systems.

The calculated frontier orbital energies of all the BINs and BIAs are summarized in Figure 2 and Table 1. As expected, all the BIAs showed higher HOMO and lower LUMO energies relative to BINs and IF, which led to a decreased bandgap (ΔE^{Th}) in line with the extended π conjugation. Both HOMO and LUMO are spread over the entire BIN/BIA backbone (Figure 2). Their topologies are qualitatively similar for both series, regardless of the cyclization direction. A noticeable contribution from the sp^3 carbon of six-membered ring containing (5,6) and (6,6) isomers to the HOMO and LUMO can be attributed to a hyperconjugation effect.

Table 1. Experimental redox and DFT calculated properties of BINs and BIAs.

Sample	E_{1ox}^0 [V] ^[a]	E_{2ox}^0 [V] ^[a]	HOMO ^[b] [eV]	LUMO ^[c] [eV]	$\Delta E^{\text{op}}\text{[d]}$ [eV]	Theoretical [eV] HOMO	Theoretical [eV] LUMO	ΔE^{Th} [eV]
2,6-N	0.83	1.28	-5.6	-2.3	3.27	-5.14	-1.28	3.86
2,6-A	0.64	1.19	-5.4	-2.6	2.81	-4.89	-1.72	3.17
1,5-N(5,6)	0.72	1.21	-5.5	-2.3	3.15	-5.17	-1.43	3.74
1,5-N(6,6)	0.81	1.24	-5.6	-2.5	3.09	-5.15	-1.45	3.70
1,5-A(5,5) ^[e]	0.62	-	-5.4	-2.6	2.76	-4.92	-1.79	3.13
1,5-A(6,6)	0.49	1.07	-5.3	-2.7	2.61	-4.85	-1.82	3.03

[a] Redox potentials versus ferrocene (Fc), in 0.2 M Bu_4NPF_6 in CH_2Cl_2 . [b] Calculated from the half-wave oxidation potentials using the equation $\text{HOMO} = -4.8 + E_{\text{1ox}}^0$ vs. Fc/Fc⁺. [c] Calculated as $\text{LUMO} = [\text{HOMO} + \Delta E^{\text{op}}]$. [d] Calculated from the red edge of the absorption spectra. [e] Recorded in 1,2-dichloroethane.

Optical properties

The absorption and emission spectra of BIN/BIA derivatives in dilute CHCl_3 solutions are shown in Figure 3 and the derived photophysical data are summarized in Table 2, along with the literature data for other IF derivatives. The absorption spectra of these chromophores are substantially (11–110 nm) redshifted relative to IF a1 ($\lambda_{\text{max}} = 347$ nm),^[16e] which can be attributed

Table 2. Photophysical data of BINs and BIAs in CHCl_3 in comparison with the literature data for IFs.

Sample	λ_{abs} [nm]	λ_{em} [nm]	Stokes shift [cm ⁻¹]	$\Phi_{\text{f}}^{[a]}$	τ_{f} [ns]	$k_{\text{f}}^{[b]}$ [10 ⁸ s ⁻¹]	$k_{\text{nr}}^{[c]}$ [10 ⁸ s ⁻¹]	Radical cation λ_{abs} [nm]
IF a1 ^{[16e][d]}	347	353	490	38	2.0	1.9	3.1	–
IF a2 ^{[14a][e]}	322	326	381	61	1.2	4.9	3.1	–
IF a3 ^{[14d][e]}	333	338	444	23	2.7	0.3	1.0	–
IF a4 ^{[14d][e]}	342	344	170	54	3.9	1.4	1.2	–
IF a5 ^{[14e][e]}	338	343	431	–	7.0	–	–	–
BIA b8 ^{[25a][f]}	488	518	1186	–	–	–	–	–
2,6-N-CH ₃	358, 372 sh	382	700 ^[g]	30	2.1	1.4	3.3	456, 494, 523, 803, 1093, 1284
2,6-A-CH ₃	432	440	420	22	3.6	0.6	2.2	575, 624, 683, 1056, 1234
1,5-N(5,6)	381	399	1184	70	1.6	4.4	1.9	434, 560, 593, 836, 1055, 1233
1,5-N(6,6)	388	404	1021	72	1.8	4.0	1.6	429, 532, 571, 857, 1084, 1258
1,5-A(5,5) ^[h]	436	447	564	41	3.5	1.1	1.7	poor solubility, not measured
1,5-A(6,6)	460	471	508	32	3.2	1.0	2.1	631, 692, 766, 1092, 1268

[a] The relative quantum yields (Φ) were measured using standard procedures with reference to 9,10-diphenylanthracene in cyclohexane ($\Phi = 0.9$).^[30] [b] $k_{\text{f}} = \Phi_{\text{f}}/\tau_{\text{f}}$. [c] $k_{\text{nr}} = 1/\tau_{\text{f}} - k_{\text{f}}$. [d] R=tolyl, measured in CH_2Cl_2 . [e] R=spirofluorene, measured in THF. [f] R=Me and *p*-decylphenyl. [g] Assuming the shoulder is a (0,0) transition, a nominal Stokes shift between the absorption/emission peak maxima is 1755 cm⁻¹. [h] Measured in 1,1,2,2-tetrachloroethane.

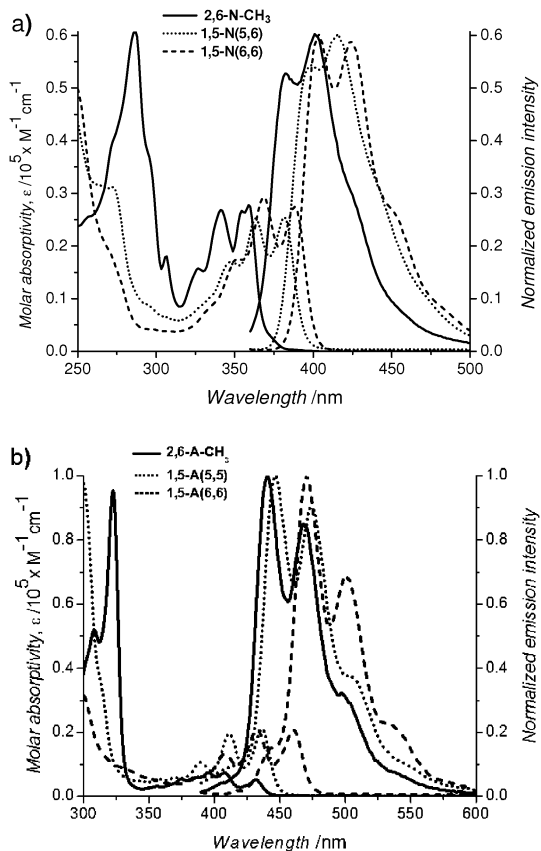


Figure 3. Absorption and emission spectra of a) BINs and b) BIAs.

to the extension of π conjugation. Both BINs and BIAs display characteristic vibronic splitting ($\approx 1400 \text{ cm}^{-1}$), indicative of the rigidity of their structure, in accordance with the previously reported IFs.^[15]

The connectivity of the terminal benzene rings with the acene core has a significant effect on optical properties, in line with the previous reports for IFs **a1–a5**. The absorption and emission bands of 1,5-BINs/BIAs are redshifted relative to their 2,6-isomers by 4–30 nm, which suggests a more effective electronic communication through the acene moiety via 1,5-positions compared to 2,6-positions. Also, comparison with the known analogue **b8** suggests a further enhancement of conjugation through 9,10-positions.^[25a] A similar effect was observed by us recently for structurally related distyrylanthracene isomers,^[29] and was rationalized by smaller bond-length alternation along the 9,10- vs 1,5- vs 2,6-pathway. Appreciable electronic effects were also noticed in regioisomers of 1,5-BIN and 1,5-BIA with identical π -electron structure but different fusion (five- versus six-membered rings). The absorption spectrum of **1,5-N(6,6)** was redshifted relative to **1,5-N(5,6)** by 10 nm, and **1,5-A(6,6)** exhibited a greater redshift of 27 nm relative to **1,5-A(5,5)**. This observation could most likely be attributed to combined consequences of distortion of the acene ring and a hyperconjugation effect (see above) in (5,6) and (6,6) isomers. We note, however, that a blueshift was observed earlier for the sterically congested IFs **a2** and **a3** compared with unhindered **a1** and **a4** with the same π -electron structure (Table 2).^[14a]

The optical gaps of BINs and BIAs deduced from the red edge of absorption spectra are in the range of approximately 3.2–3.5 and 2.7–2.9 eV, respectively. The optical gap contraction by about 0.5 and 0.8 eV observed in BIAs relative to BINs and IF, respectively, is brought about by a raised HOMO and lowered LUMO (see above), a result of extended π conjugation.

All compounds exhibited intense blue to cyan fluorescence with vibronically split bands at approximately 380–430 and 440–500 nm for BINs and BIAs, respectively. The Stokes shifts are small, consistent with the planar and rigid structure of the molecules. However, the observed trend of the Stokes shift: BINs > BIAs ~ IF (490 cm^{-1}) (Table 2) does not follow the extension of π conjugation. The most likely explanation lies in the change of the exciton delocalization: a full delocalization between three benzene rings in IF, to partial localization of the central naphthalene or anthracene core in BINs and BIAs, respectively. The emission quantum yield (ϕ_f) of BIN isomers (30–72%) is consistently higher than that of BIAs (22–41%) and in both series, the 1,5-substituted derivatives showed high quantum yields (32–72%) relative to 2,6-congeners (22–30%). Analysis of radiation lifetimes suggests that both trends could be attributed to faster radiative decay of the naphthalene versus anthracene derivatives, and of 1,5- versus 2,6-isomers, although the structural reason behind this is not immediately clear. The nonradiative decay rates are similar for BIN/BIA derivatives, as can be expected based on their highly rigid structure.

Electrochemical properties

The electrochemical properties of all BINs and BIAs were measured in CH_2Cl_2 solution by cyclic voltammetry and the corresponding data are summarized in Table 1. Figure 4 shows the representative cyclic voltammograms of **1,5-N(5,6)** and **1,5-N(6,6)**. All BIN and BIA derivatives feature one single-electron reversible oxidation wave, followed by a second, irreversible multielectron oxidation. The first oxidation potential decreases in the range IF (1.44 V vs. Ag/AgCl for **a1**,^[16a] ca. 1.0 V vs. Fc/Fc⁺) to BIN (≈ 0.8 V vs. Fc/Fc⁺) to BIA (≈ 0.6 V vs. Fc/Fc⁺), consistent with the extension of π conjugation. From the half-wave oxidation potentials, HOMO levels were determined. The

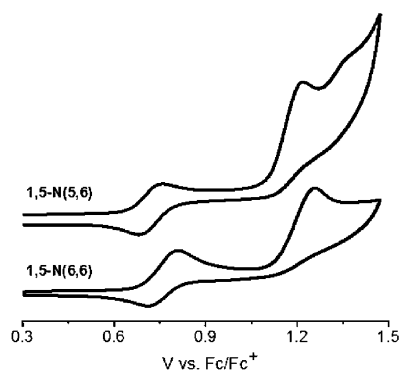


Figure 4. Cyclic voltammograms of **1,5-N(5,6)** and **1,5-N(6,6)** in 0.2 M Bu_4NPF_6 in CH_2Cl_2 .

estimated HOMO level is progressively raised from IF (≈ -5.9 eV) to the BINs (-5.5 – -5.6 eV) and BIAs (≈ -5.3 – -5.4 eV), which might be useful for reducing the hole injection barrier in organic electronic devices.

Due to the large HOMO–LUMO gap of these compounds, no reduction was observed within the electrochemical window of the solvent (-2.3 – $+1.7$ V vs. Fc/Fc $^+$). The LUMO energies were thus approximated by adding the optical gap to the electrochemically determined HOMO level. Comparing these experimental HOMO and LUMO values with the calculated ones suggests that DFT overestimates the energy of frontier orbitals by approximately 0.4 eV for the HOMO and approximately 0.9 eV for the LUMO and, as a result, slightly overestimates the gap. However, all the discussed trends in electronic energies are reproduced well by the calculations.

Spectroelectrochemistry

Open-shell radical cations, formed in the above-discussed one-electron oxidation, act as charge carriers in organic electronic devices in which their chemical and thermodynamic stability plays a crucial role. Therefore, studies of the electronic structure and stability of these species are essential for designing efficient optoelectronic materials. The UV/Vis–near-infrared (NIR) spectra of radical cations of BIN and AIN formed by *in situ* oxidation in a spectroelectrochemical cell are shown in Figure 5. Upon applying the progressively increasing anodic potential, the intense absorption band at 380/400 nm of the neutral molecules attenuates while the new absorption bands concomitantly grow in the Vis and NIR range of the spectrum (Table 2). Clear isosbestic points (e.g., 333 and 362 nm for **2,6-N-CH₃**; 328, 428, and 438 nm for **2,6A-CH₃**) indicate that only two interconverting species (neutral and radical cation) are present over the course of the oxidation.

The newly appearing absorption in the visible range (450–650 nm) can be assigned to the SOMO-to-LUMO transitions, whereas the NIR bands (> 700 nm) are due to HOMO-to-SOMO transitions.^[31] Such attribution is in line with the asymmetric position of the SOMO in the HOMO–LUMO gap of radical cations, for example, **2,6A-CH₃**: HOMO (-8.4 eV), SOMO (-8.0 eV), LUMO (-5.0 eV) (gas-phase calculations; the absolute energies in solution would be significantly different). Surprisingly, the first NIR absorption band of BIA radical cations shows no pronounced redshift versus that of BIN radical cations (slight redshift for 1,5-isomers; slight blueshift for 2,6-isomers), although the expected redshift is observed for the new absorption band in the visible range. This could likely be attributed to a more pronounced solvent/electrolyte stabilization of the smaller (less delocalized) radical cation of BIN relative to BIA.^[32]

Application of a mild reductive potential of -100 mV quantitatively transforms the radical cations back to the neutral state, as manifested by the complete disappearance of the long-wavelength absorption and full recovery of the original spectrum.

This redox interconversion is also manifested in a characteristic color change, from the colorless neutral state to crimson red for **1,5-N(5,6)** and deep purple for **1,5-N(6,6)** in the cation

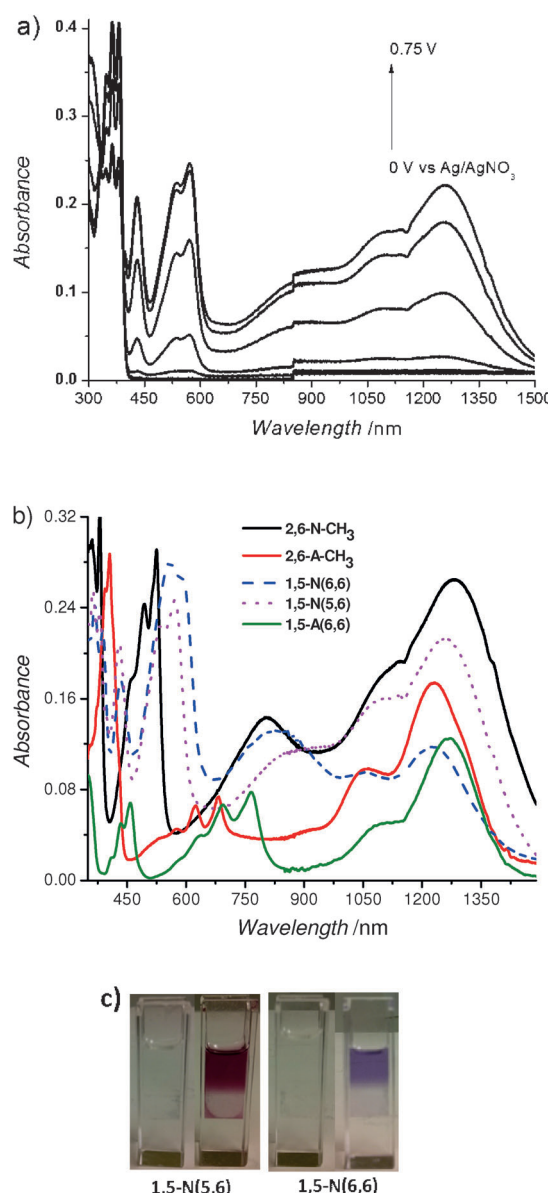


Figure 5. Spectroelectrochemical spectra of **1,5-N(5,6)** (a) and overlaid absorption spectra of four cation radicals (b). c) Photograph of 1,5-BIN solutions in the neutral (left) and radical cation (right) state.

radical state. Such a property, along with the high stability of the oxidized form, makes these materials of potential interest for electrochromic devices.^[33]

Conclusion

We have synthesized π -extended IF analogues (BINs/BIAs) through a high-yield acid-catalyzed cyclization of naphthalene and anthracene precursors. The effect of regioisomerism on the structural, optical, and electrochemical properties of these compounds has been studied experimentally and computationally. Crystallographic analysis and DFT calculations reveal that the conjugated backbone of (5,5) isomers is nearly planar, whereas a considerable distortion is present in the (5,6) and (6,6) isomers. Compared with the parent IF, the extended

acene core endows redshifted absorption and emission spectra and lowered oxidation potentials. An electrochemical oxidation of all regioisomers led to reversible formation of the corresponding radical cations. An associated color change and new characteristic absorption bands in the visible and NIR region of the spectrum make these materials of potential interest for electrochromic devices. Future work will focus on application of BIN/BIA derivatives as monomers for emissive conjugated polymers and their use in optoelectronic devices.

Experimental Section

Materials and methods

All chemicals were used as received unless otherwise noted. UV/Vis/NIR absorption spectra were obtained using a JASCO V-670 spectrophotometer and fluorescence spectra were acquired using a Cary Eclipse spectrophotometer. Lifetime measurements were done with an Edinburgh Instruments Mini Tau lifetime fluorimeter with an EPL 405 laser (excited at 405 nm). All electrochemical experiments were performed at room temperature with a CHI-770 electrochemical workstation. Spectroelectrochemical experiments were carried out in a thin-layer quartz cuvette containing a Pt mesh working electrode, a platinum wire counter electrode, and a Ag/AgNO₃ reference electrode. Cyclic voltammetry measurements were performed in 0.2 M tetrabutylammonium hexafluorophosphate solution in CH₂Cl₂ (or 1,2-dichloroethane) with a Pt disk as a working electrode, Ag/AgNO₃ as a reference electrode, and a Pt wire as a counter electrode. Scan rates were 100 mV s⁻¹ and ferrocene was added at the end of experiments as an internal standard. DFT calculations of the optimized molecular structures (in the gas phase) and the molecular orbital energies were carried out at the B3LYP/6-31G(d) level as implemented in Gaussian 09.^[34] Unrestricted UB3LYP/6-31G(d) was used for cation radicals. Frequency calculations were performed for all isomers with distorted aromatic core and showed no negative frequencies. The molecular orbital surfaces were generated with GaussView 5.0. CCDC 1041229 (**1,5-A(5,5)**), 1041230 (**1,5-N(6,6)**), and 1041231 (**2,6-A(CH₃)** endoperoxide) contain the supplementary crystallographic data for this paper. These data can be obtained free of charge from The Cambridge Crystallographic Data Centre via www.ccdc.cam.ac.uk/data_request/cif.

Syntheses

All reactions were performed under an inert atmosphere (N₂).

Synthesis of 2a–2d: A dioxane solution of 2-ethoxycarbonylphenylboronic acid (1.16 g, 6.0 mmol), K₃PO₄ (4.07 g, 19.2 mmol), Pd(PPh₃)₄ (69 mg, 0.06 mmol), and **1a–1d** (2.4 mmol) was heated at reflux at 100 °C for 24 h. After cooling to 20 °C, a saturated aqueous solution of NH₄Cl was added. The organic layer was extracted with ethyl acetate and dried (MgSO₄), filtered, and the filtrate was concentrated in vacuo. The residue was purified by silica column chromatography (1:3 hexane/CH₂Cl₂) to yield the desired compounds.

2a: White powder (63%, 0.64 g); ¹H NMR (400 MHz, CDCl₃): δ = 7.90 (d, *J* = 7.2 Hz, 2H), 7.87 (d, *J* = 8.4 Hz, 2H), 7.88 (s, 2H), 7.59–7.55 (m, 2H), 7.49–7.43 (m, 6H), 4.09 (q, *J* = 7.2 Hz, 4H), 0.92 ppm (t, *J* = 7.2 Hz, 6H); ¹³C NMR (125 MHz, CDCl₃): δ = 168.8, 142.3, 139.2, 132.3, 131.4, 131.3, 131.0, 129.9, 127.5, 127.5, 127.3, 126.7, 61.0, 13.7 ppm; IR: ν = 2981 (C—H), 1710 (C=O), 1596, 1444,

1361 cm⁻¹; HRMS: *m/z* calcd for C₂₈H₂₄O₄: 447.1566 [M + Na]; found: 447.1548

2b: Light yellow powder (67%, 0.75 g); ¹H NMR (400 MHz, CDCl₃): δ = 8.44 (s, 2H), 8.02 (d, *J* = 8.6 Hz, 2H), 7.95 (s, 2H), 7.91 (d, *J* = 7.6 Hz, 2H), 7.61–7.58 (m, 2H), 7.55–7.53 (m, 2H), 7.55–7.53 (m, 2H), 7.49–7.43 (m, 4H), 4.08 (q, *J* = 7.2 Hz, 4H), 0.89 ppm (t, *J* = 7.2 Hz, 6H); ¹³C NMR (125 MHz, CDCl₃): δ = 168.8, 142.4, 138.7, 131.6, 131.4, 131.3, 131.0, 130.9, 130.0, 127.6, 127.4, 127.3, 126.8, 126.3, 61.0, 13.7 ppm; IR: ν = 2978 (C—H), 1712 (C=O), 1594, 1480 cm⁻¹; HRMS: *m/z* calcd for C₃₂H₂₆O₄: 475.1909 [M + H]; found: 475.1905.

2c: White powder (66%, 0.67 g); ¹H NMR (400 MHz, CDCl₃; observed two rotamers): δ = 8.08 (m, 2H), 7.66 (m, 4H), 7.58 (m, 4H), 7.44 (m, 4H), 7.30 (m, 2H), 7.85 (m, 4H), 7.30 (d, *J* = 6.4 Hz, 2H), 4.09–3.81 (m, 4H), 0.86 (t, *J* = 7.2 Hz, 2H), 0.62 ppm (t, *J* = 7.2 Hz, 4H); ¹³C NMR (125 MHz, CDCl₃): δ = 167.7, 167.5, 141.4, 141.3, 140.0, 139.9, 132.1, 132.0, 131.98, 131.92, 131.7, 131.4, 131.3, 130.1, 130.0, 127.6, 127.5, 125.9, 125.7, 125.2, 125.1, 60.6, 60.5, 13.6, 13.1 ppm; IR: ν = 2976 (C—H), 1702 (C=O), 1597, 1473, 1404 cm⁻¹; HRMS: *m/z* calcd for C₂₈H₂₄O₄: 447.1566 [M + Na]; found: 447.1549.

2d: Light yellow powder (45%, 0.51 g); ¹H NMR (400 MHz, CDCl₃; observed two rotamers): δ = 8.10–8.00 (m, 4H), 7.86–7.84 (m, 2H), 7.71–7.66 (m, 2H), 7.62–7.59 (m, 2H), 7.56–7.42 (m, 4H), 7.28–7.25 (m, 2H), 3.82–3.68 (m, 4H), 1.00–0.46 ppm (m, 6H); IR: ν = 2979 (C—H), 1705 (C=O), 1597, 1442 cm⁻¹; HRMS: *m/z* calcd for C₃₂H₂₆O₄: 475.1909 [M + H]; found: 475.1915.

Synthesis of BINs and BIAs: A solution of 4-bromotoluene (0.68 mL, 5.6 mmol) in THF (10 mL) was cooled to –78 °C and nBuLi (2.21 mL of 2.5 M solution, 5.5 mmol) was added. After stirring at –78 °C for 1 h, a solution of **2a–2d** (0.56 mmol) in THF (10 mL) was added slowly and the reaction mixture was then warmed to room temperature and stirred for 1 h before being quenched with water. The organic layer was extracted with ethyl acetate, dried over MgSO₄, and concentrated in vacuo. The crude product was washed with hexane and used directly in the cyclization step. Trifluoroacetic acid (5 mL) was added to the flask containing intermediates **3a–3d** (0.20 mmol) and the mixture was stirred at room temperature for 2 h. The resultant solution was poured into water (100 mL). The mixture was extracted with dichloromethane and the combined organic extracts were dried over MgSO₄ and concentrated. The residues were purified by flash silica gel column chromatography (1:1 hexanes/CH₂Cl₂) followed by washing with hexanes.

2,6-N-CH₃: White powder (230 mg, 60%); ¹H NMR (400 MHz, CDCl₃): δ = 7.95 (d, *J* = 8.4 Hz, 2H), 7.78 (d, *J* = 8.8 Hz, 2H), 7.70 (d, *J* = 7.2 Hz, 2H), 7.41 (d, *J* = 7.6 Hz, 2H), 7.32 (dd, ¹*J* = 7.2, 0.8 Hz, 2H), 7.23 (d, *J* = 8.4 Hz, 8H), 7.18 (dd, *J* = 7.2, 1.2 Hz, 2H), 7.05 (d, *J* = 8.4 Hz, 8H), 2.30 ppm (s, 12H); ¹³C NMR (125 MHz, CDCl₃): δ = 155.8, 147.6, 140.2, 140.0, 137.3, 136.1, 130.4, 129.2, 128.8, 127.6, 127.1, 126.9, 125.0, 119.4, 118.7, 65.8, 21.0 ppm; IR: ν = 2970 (C—H), 1508, 1460, 1286, 1186, 1020, 915 cm⁻¹; UV/Vis (CHCl₃): λ_{max} (ε) = 285 (43 400), 341 (18 500), 358 (19 000), 372 sh nm (1400 M⁻¹ cm⁻¹); HRMS: *m/z* calcd for C₅₂H₄₀: 665.3203 [M + H]; found: 665.3191.

2,6-N-CF₃: White powder (260 mg, 53%); ¹H NMR (400 MHz, CDCl₃): δ = 7.95 (d, *J* = 8.4 Hz, 2H), 7.77 (d, *J* = 8.8 Hz, 2H), 7.70 (d, *J* = 7.6 Hz, 2H), 7.41 (d, *J* = 7.6 Hz, 2H), 7.31 (d, *J* = 7.6 Hz, 2H), 7.23 (d, *J* = 8.0 Hz, 8H), 7.19 (d, *J* = 7.6 Hz, 2H), 7.04 ppm (d, *J* = 8.0 Hz, 8H); ¹³C NMR (125 MHz, CDCl₃): δ = 153.8, 146.4, 146.0, 139.8, 138.0, 129.9, 129.3, 129.1, 128.3, 128.1, 126.8, 125.3, 124.9, 122.8, 120.0, 119.5, 65.9 ppm; IR: ν = 1616, 1408, 1323, 1163, 1069, 919 cm⁻¹; UV/Vis (CHCl₃): λ_{max} (ε) = 289 (47 200), 324 (12 400), 338 (19 200),

352 nm (20200 M⁻¹ cm⁻¹); HRMS: *m/z* calcd for C₅₂H₂₈F₁₂: 880.2005 [M⁺]; found: 880.1998.

2,6-A-CH₃: Light yellow powder (220 mg, 57%); ¹H NMR (400 MHz, CDCl₃): δ = 8.35 (s, 2H), 7.88 (d, *J* = 8.4 Hz, 2H), 7.85 (d, *J* = 8.4 Hz, 2H), 7.79 (d, *J* = 7.6 Hz, 2H), 7.47 (d, *J* = 7.6 Hz, 2H), 7.36 (td, *J* = 7.2 Hz, ²*J* = 0.8 Hz, 2H), 7.26 (d, *J* = 8.4 Hz, 8H), 7.23 (d, *J* = 7.62 Hz, 2H), 7.02 (d, *J* = 8.0 Hz, 8H), 7.27 ppm (s, 12H); ¹³C NMR (125 MHz, CDCl₃): δ = 156.2, 146.0, 140.4, 140.0, 137.4, 136.2, 132.3, 130.6, 129.1, 128.8, 127.5, 127.2, 127.1, 125.8, 124.9, 119.4, 118.6, 65.7, 21.0 ppm; IR: $\tilde{\nu}$ = 2961 (C—H), 1508, 1441, 1258, 1186, 1016, 915 cm⁻¹; UV/Vis (CHCl₃): λ_{max} (ϵ) = 305 (70400), 322 (138600), 373 (6000), 395 (8100), 407 (8700), 432 nm (6600 M⁻¹ cm⁻¹); HRMS: *m/z* calcd for C₅₆H₄₃: 715.3365 [M + H]; found: 715.3388.

2,6-A-CF₃: Light yellow powder (290 mg, 56%); ¹H NMR (400 MHz, CDCl₃): δ = 8.18 (s, 2H), 7.96 (d, *J* = 8.8 Hz, 2H), 7.92 (d, *J* = 8.4 Hz, 2H), 7.87 (d, *J* = 7.6 Hz, 2H), 7.51 (d, *J* = 8.8 Hz, 8H), 7.47 (m, 10H), 7.43 (d, *J* = 7.2 Hz, 8H), 7.32 ppm (dd, *J* = 7.6, 0.8 Hz, 2H); ¹³C NMR (125 MHz, CDCl₃): δ = 154.3, 146.3, 144.0, 140.2, 138.3, 132.3, 131.3, 129.4, 129.3, 129.1, 128.1, 126.8, 125.38, 125.35, 125.30, 124.8, 120.1, 119.1, 65.6 ppm; IR: $\tilde{\nu}$ = 1614, 1411, 1322, 1169, 1109, 920 cm⁻¹; UV/Vis (CHCl₃): λ_{max} (ϵ) = 307 (69600), 321 (140000), 375 (5800), 395 (8000), 408 (8600), 430 nm (6740 M⁻¹ cm⁻¹); HRMS: *m/z* calcd for C₅₆H₃₁F₁₂: 931.2229 [M + H]; found: 931.2210.

1,5-N(6,6): White powder (120 mg, 32%); ¹H NMR (500 MHz, CDCl₃): δ = 8.02 (m, 4H), 7.35 (t, *J* = 7.0 Hz, 2H), 7.24 (t, *J* = 7.5 Hz, 2H), 7.15 (m, 4H), 7.00 (d, *J* = 8.0 Hz, 8H), 6.87 (d, *J* = 8.5 Hz, 8H), 2.31 ppm (s, 12H); ¹³C NMR (125 MHz, CDCl₃): δ = 144.9, 142.8, 142.1, 135.7, 132.8, 131.1, 130.3, 128.6, 128.5, 128.3, 127.6, 126.9, 126.8, 123.7, 119.5, 59.3, 20.9 ppm; IR: $\tilde{\nu}$ = 2917 (C—H), 1574, 1449, 1397, 1195, 1021, 912 cm⁻¹; UV/Vis (CHCl₃): λ_{max} (ϵ) = 272 (12200), 345 (11500), 368 (19600), 388 nm (18900 M⁻¹ cm⁻¹); HRMS: *m/z* calcd for C₅₂H₄₀: 665.3208 [M + H]; found: 665.3203.

1,5-N(5,6): White powder (80 mg, 21%); ¹H NMR (500 MHz, CDCl₃): δ = 8.75 (d, *J* = 8.5 Hz, 1H), 8.35 (d, *J* = 7.5 Hz, 1H), 8.16 (d, *J* = 7.5 Hz, 1H), 8.11 (d, *J* = 8.0 Hz, 1H), 7.70 (t, *J* = 7.5 Hz, 1H), 7.47 (m, 3H), 7.38 (t, *J* = 7.0 Hz, 1H), 7.31 (d, *J* = 7.5 Hz, 1H), 7.21 (t, *J* = 7.5 Hz, 1H), 7.04 (d, *J* = 8.0 Hz, 4H), 6.99 (d, *J* = 8.0 Hz, 4H), 6.92 (m, 5H), 6.80 ppm (d, *J* = 8.5 Hz, 4H); ¹³C NMR (125 MHz, CDCl₃): δ = 152.4, 150.1, 145.0, 142.5, 142.4, 142.1, 141.2, 136.2, 135.5, 133.1, 132.8, 131.4, 131.1, 130.2, 129.6, 128.8, 128.1, 128.1, 127.6, 127.5, 127.2, 127.0, 126.8, 126.7, 126.4, 126.1, 124.3, 123.9, 123.2, 119.5, 64.9, 59.7, 21.0, 20.9 ppm; IR: $\tilde{\nu}$ = 2916 (C—H), 1575, 1445, 1395, 1261, 1185, 1018, 913 cm⁻¹; UV/Vis (CHCl₃): λ_{max} (ϵ) = 273 (2100), 349 (11200), 363 (16900), 381 nm (17000 M⁻¹ cm⁻¹); HRMS: *m/z* calcd for C₅₂H₄₀: 665.3208 [M + H]; found: 665.3203.

1,5-A(5,5): Light yellow powder (210 mg, 54%); ¹H NMR (400 MHz, C₂D₂Cl₄): δ = 9.36 (s, 2H), 8.55 (d, *J* = 7.0 Hz, 2H), 8.14 (d, *J* = 7.5 Hz, 2H), 7.62 (d, 2H), 7.54 (m, 4H), 7.36 (t, *J* = 8.5 Hz, 2H), 7.14 (d, *J* = 8.5 Hz, 8H), 7.04 (d, *J* = 8.5 Hz, 8H), 2.31 ppm (s, 12H); ¹³C NMR (125 MHz, C₂D₂Cl₄): δ = 153.0, 150.0, 141.6, 141.2, 136.3, 133.7, 132.3, 129.3, 128.9, 128.1, 127.4, 127.3, 126.7, 125.8, 123.9, 122.9, 120.1, 64.7, 20.9 ppm; IR: $\tilde{\nu}$ = 2919 (C—H), 1596, 1508, 1446, 1407, 1182, 1160, 1037, 914 cm⁻¹; UV/Vis (C₂D₂Cl₄): λ_{max} (ϵ) = 388 (14100), 411 (26900), 436 nm (28200 M⁻¹ cm⁻¹); HRMS: *m/z* calcd for C₅₆H₄₃: 715.3365 [M + H]; found: 715.3385.

1,5-A(6,6): Light yellow powder (3 mg, 1%); ¹H NMR (400 MHz, CDCl₃): δ = 7.78 (d, *J* = 8.2 Hz, 1H), 7.69 (m, 4H), 7.23 (t, *J* = 8.0 Hz, 2H), 7.13 (d, *J* = 8.2 Hz, 2H), 7.08 (d, *J* = 7.6 Hz, 8H), 7.00 (m, 10H), 6.86 (dd, *J* = 8.2, 1.2 Hz, 1H), 2.20 ppm (s, 8H); IR: $\tilde{\nu}$ = 2917 (C—H), 1506, 1446, 1259, 1194, 1160, 1019, 916 cm⁻¹; UV/Vis (CHCl₃): λ_{max} (ϵ) = 408 (22600), 432 (27900), 460 nm (28000 M⁻¹ cm⁻¹); HRMS: *m/z* calcd for C₅₆H₄₃: 715.3365 [M + H]; found: 715.3384.

Acknowledgements

This work was supported by NSERC and NanoQuebec. M.R.R. acknowledges the PBEEE postdoctoral fellowship from FQRNT.

Keywords: acenes • conjugation • fused-ring systems • indenofluorenes • organic electronics

- [1] a) *Functional Organic Materials* (Eds. T. J. J. Muller and U. H. F. Bunz), Wiley-VCH, Weinheim, Germany, **2007**; b) *Carbon-Rich Compounds* (Eds. M. M. Haley and R. R. Tykwinski), Wiley-VCH, Weinheim, Germany, **2006**; c) *Organic Electronics II* (Ed. H. Klauk), Wiley-VCH, Weinheim, Germany, **2012**; d) *Chem. Rev.* **2007**, *107*, 922–1386 (Thematic issue: Organic Electronics and Optoelectronics); e) *Chem. Mater.* **2011**, *23*, 309–922 (Thematic issue: π -Functional Materials).
- [2] a) G. Rieveschl, F. E. Ray, *Chem. Rev.* **1938**, *23*, 287–389; b) T. P. I. Saragi, T. Spehr, A. Siebert, T. Fuhrmann-Lieker, J. Salbeck, *Chem. Rev.* **2007**, *107*, 1011–1065; c) J. U. Wallace, S. H. Chen, *Adv. Polym. Sci.* **2008**, *212*, 145–186; d) I. V. Kurdyukova, A. A. Ishchenko, *Russ. Chem. Rev.* **2012**, *81*, 258–290.
- [3] a) M. T. Bernius, M. Inbasekaran, J. O'Brien, W. Wu, *Adv. Mater.* **2000**, *12*, 1737–1750; b) D. Y. Kim, H. N. Cho, C. Y. Kim, *Prog. Polym. Sci.* **2000**, *25*, 1089–1139; c) D. neher, *Macromol. Rapid Commun.* **2001**, *22*, 1365–1385; d) M. Leclerc, *J. Polym. Sci. Part A* **2001**, *39*, 2867–2873; e) U. Scherf, E. J. W. List, *Adv. Mater.* **2002**, *14*, 477–487.
- [4] a) R. Xia, G. Heliotis, D. C. Bradley, *Appl. Phys. Lett.* **2003**, *82*, 3599–3601; b) G. Heliotis, R. Xia, G. A. Turnbull, P. Andrew, W. L. Barnes, I. D. W. Samuel, D. C. Bradley, *Adv. Funct. Mater.* **2004**, *14*, 91–97; c) I. D. W. Samuel, G. A. Turnbull, *Mater. Today* **2004**, *7*, 28–35; d) I. D. W. Samuel, G. A. Turnbull, *Chem. Rev.* **2007**, *107*, 1272–1295.
- [5] R. Mondal, N. Miyaki, H. A. Becerril, J. E. Norton, J. Parmer, A. C. Mayer, M. L. Tang, J.-L. Brédas, M. D. McGehee, Z. Bao, *Chem. Mater.* **2009**, *21*, 3618–3362.
- [6] a) J. M. Halls, A. C. Arias, J. D. MacKenzie, W. S. Wu, M. Inbasekaran, E. P. Woo, R. H. Friend, *Adv. Mater.* **2000**, *12*, 498–502; b) O. Inganäs, F. Zhang, M. R. Anderson, *Acc. Chem. Res.* **2009**, *42*, 1731–1739.
- [7] a) U. J. Scherf, *J. Mater. Chem.* **1999**, *9*, 1853–1864; b) A. C. Grimsdale, K. Müllen, *Angew. Chem. Int. Ed.* **2005**, *44*, 5592–5629; *Angew. Chem.* **2005**, *117*, 5732–5772.
- [8] a) S. Setayesh, D. Marsitzky, K. Müllen, *Macromolecules* **2000**, *33*, 2016–2020; b) J. Jacob, J. Zhang, A. C. Grimsdale, K. Müllen, M. Gaal, E. J. W. List, *Macromolecules* **2003**, *36*, 8240–8245.
- [9] D. Hertel, U. Scherf, H. Bässeler, *Adv. Mater.* **1998**, *10*, 1119–1122.
- [10] a) A. C. Grimsdale, K. L. Chan, R. E. Martin, P. G. Jokisz, A. B. Holmes, *Chem. Rev.* **2009**, *109*, 897–1091.
- [11] a) W. Zhang, J. Smith, R. Hamilton, M. Heeney, J. Kirkpatrick, K. Song, S. E. Watkins, T. Anthopoulos, I. McCulloch, *J. Am. Chem. Soc.* **2009**, *131*, 10814–10815; b) H. Usta, C. Risko, Z. Wang, H. Huang, M. K. Deliomeroğlu, A. Zhukhovitskiy, A. Facchetti, T. J. Marks, *J. Am. Chem. Soc.* **2009**, *131*, 5586–5608.
- [12] Q. Zheng, B. J. Jung, J. Sun, H. E. Katz, *J. Am. Chem. Soc.* **2010**, *132*, 5394–5404.
- [13] L.-C. Chi, W.-Y. Hung, H.-C. Chiu, K.-T. Wong, *Chem. Commun.* **2009**, 3892–3894.
- [14] a) D. Thirion, C. Poriol, J. Rault-Berthelot, F. Barrière, O. Jeannin, *Chem. Eur. J.* **2010**, *16*, 13646–13658; b) C. Poriol, R. Métivier, J. Rault-Berthelot, D. Thirion, F. Barrière, O. Jeannin, *Chem. Commun.* **2011**, *47*, 11703–11705; c) D. Thirion, M. Romain, J. Rault-Berthelot, C. Poriol, *J. Mater. Chem.* **2012**, *22*, 7149–7157; d) M. Romain, D. Tondelier, J.-C. Vanel, B. Geffroy, O. Jeannin, J. Rault-Berthelot, R. Métivier, C. Poriol, *Angew. Chem. Int. Ed.* **2013**, *52*, 14147–14151; *Angew. Chem.* **2013**, *125*, 14397–14401; e) M. Romain, S. Thiery, A. Shirinskaya, C. Declairieux, D. Tondelier, B. Geffroy, O. Jeannin, J. Rault-Berthelot, R. Métivier, C. Poriol, *Angew. Chem. Int. Ed.* **2015**, *54*, 1176–1180; *Angew. Chem.* **2015**, *127*, 1192–1196.
- [15] a) T. Hadizad, J. Zhang, Z. Y. Wang, T. C. Gorjanc, C. Py, *Org. Lett.* **2005**, *7*, 795–797; b) L. A. Estrada, V. A. Montes, G. Zyryanov, P. Anzenbacher Jr,

- J. Phys. Chem. B* **2007**, *111*, 6983–6986; c) D. Thirion, J. Rault-Berthelot, L. Vignau, C. Poriel, *Org. Lett.* **2011**, *13*, 4418–4421.
- [16] a) K.-T. Wong, L.-C. Chi, S.-C. Huang, Y.-L. Liao, Y.-H. Liu, Y. Wang, *Org. Lett.* **2006**, *8*, 5029–5032; b) Y. Wu, J. Zhang, Z. Bo, *Org. Lett.* **2007**, *9*, 4435–4438; c) N. Cocherel, C. Poriel, J. Rault-Berthelot, F. Barrière, N. Audebrand, A. M. Z. Slawin, L. Vignau, *Chem. Eur. J.* **2008**, *14*, 11328–11342; d) C. Poriel, N. Cocherel, J. Rault-Berthelot, L. Vignau, O. Jeannin, *Chem. Eur. J.* **2011**, *17*, 12631–12645; e) H.-H. Huang, Ch. Prabhakar, K.-C. Tang, P.-T. Chou, G.-J. Huang, J.-S. Yang, *J. Am. Chem. Soc.* **2011**, *133*, 8028–8039.
- [17] a) C. Poriel, J. Rault-Berthelot, D. Thirion, F. Barrière, L. Vignau, *Chem. Eur. J.* **2011**, *17*, 14031–14046; b) D. Thirion, C. Poriel, R. Mtivier, J. Rault-Berthelot, F. Barrière, O. Jeannin, *Chem. Eur. J.* **2011**, *17*, 10272–10287; c) C. Poriel, J.-J. Liang, J. Rault-Berthelot, F. Barrière, N. Cocherel, A. M. Z. Slawin, D. Horhart, M. Virboul, G. Alcaraz, N. Audebrand, L. Vignau, N. Huby, G. Wantz, L. Hirsch, *Chem. Eur. J.* **2007**, *13*, 10055–10069; d) C. Poriel, J. Rault-Berthelot, D. Thirion, *J. Org. Chem.* **2013**, *78*, 886–898; e) C. Poriel, J. Rault-Berthelot, F. Barrière, A. M. Z. Slawin, *Org. Lett.* **2008**, *10*, 373–376; f) G. Zhou, M. Baumgarten, K. Müllen, *J. Am. Chem. Soc.* **2007**, *129*, 12211–12221.
- [18] B. S. Nehls, D. Galbrecht, D. J. Brauer, C. W. Lehmann, U. Scherf, T. Farrell, *J. Polym. Sci. Part A* **2006**, *44*, 5533–5545.
- [19] X.-Y. Cao, W.-B. Zhang, J.-L. Wang, X.-H. Zhou, H. Lu, J. Pei, *J. Am. Chem. Soc.* **2003**, *125*, 12430–12431.
- [20] a) A. L. Kanibolotsky, R. Berridge, P. J. Skabara, I. F. Perepichka, D. C. Bradley, M. Koeberg, *J. Am. Chem. Soc.* **2004**, *126*, 13695–13702; b) K. M. Omer, A. L. Kanibolotsky, P. J. Skabara, I. F. Perepichka, A. J. Bard, *J. Phys. Chem. B* **2007**, *111*, 6612–6619; c) M. M. Oliva, J. Casado, J. T. L. Navarrete, R. Berridge, P. J. Skabara, A. L. Kanibolotsky, I. F. Perepichka, *J. Phys. Chem. B* **2007**, *111*, 4026–4035; d) N. A. Montgomery, J.-C. Denis, S. Schumacher, A. Ruseckas, P. J. Skabara, A. Kanibolotsky, M. J. Paterson, I. Galbraith, G. A. Turnbull, I. D. W. Samuel, *J. Phys. Chem. A* **2011**, *115*, 2913–2919.
- [21] a) M. Kimura, S. Kuwano, Y. Sawaki, H. Fujikawa, K. Noda, Y. Taga, K. Takagi, *J. Mater. Chem.* **2005**, *15*, 2393–2398; b) Y. Sun, K. Xiao, Y. Liu, J. Wang, J. Pei, G. Yu, D. Zhu, *Adv. Funct. Mater.* **2005**, *15*, 818–822; c) J. Luo, Y. hou, Z.-Q. Niu, Q.-F. Zhou, Y. Ma, J. Pei, *J. Am. Chem. Soc.* **2007**, *129*, 11314–11315; d) H. Xia, J. He, B. Xu, S. Wen, Y. Li, W. Tian, *Tetrahedron* **2008**, *64*, 5736–5742; e) J.-L. Wang, J. Yan, Z.-M. Tang, Q. Xiao, Y. Ma, J. Pei, *J. Am. Chem. Soc.* **2008**, *130*, 9952–9962; f) S. Gomez-Estebaran, M. Pezella, A. Domingo, G. Hennrich, B. Gmez-Lor, *Chem. Eur. J.* **2013**, *19*, 16080–16086.
- [22] a) B. D. Rose, D. T. Chase, C. D. Weber, L. N. Zakharov, M. C. Lonergan, M. M. Haley, *Org. Lett.* **2011**, *13*, 2106–2109; b) B. D. Rose, C. L. Vonnegut, L. N. Zakharov, M. M. Haley, *Org. Lett.* **2012**, *14*, 2426–2429; c) D. T. Chase, A. G. Fix, S. J. Kang, B. D. Rose, C. Weber, Y. Zhong, L. Zakharov, M. C. Lonergan, C. Nuckolls, M. M. Haley, *J. Am. Chem. Soc.* **2012**, *134*, 10349–10352; d) A. G. Fix, P. E. Deal, C. L. Vonnegut, B. D. Rose, L. N. Zakharov, M. M. Haley, *Org. Lett.* **2013**, *15*, 1362–1365.
- [23] a) A. Shimizu, Y. Tobe, *Angew. Chem. Int. Ed.* **2011**, *50*, 6906–6910; *Angew. Chem.* **2011**, *123*, 7038–7042; b) A. Shimizu, R. Kishi, M. Nakano, D. Shiomi, K. Sato, T. Takui, I. Hisaki, M. Miyata, Y. Tobe, *Angew. Chem. Int. Ed.* **2013**, *52*, 6076–6079; *Angew. Chem.* **2013**, *125*, 6192–6195.
- [24] K.-T. Wong, T.-C. Chao, L.-C. Chi, Y.-Y. Chu, A. Balaiah, S.-F. Chiu, Y.-H. Liu, Y. Wang, *Org. Lett.* **2006**, *8*, 5033–5036.
- [25] a) C. Yang, J. Jacob, K. Müllen, *Macromolecules* **2006**, *39*, 5696–5704; b) B. S. Nehls, S. Füldner, E. Preis, T. Farrell, U. Scherf, *Macromolecules* **2005**, *38*, 687–694; c) X. Guo, B. Yhao, G. Jiang, Y. Cheng, Z. Xie, L. Wang, X. Jing, F. Wang, *J. Polym. Sci. Part A* **2008**, *46*, 4866–4878.
- [26] In most electrophilic aromatic substitutions, naphthalene reacts through 1,8-positions whereas anthracene reacts through 9,10-positions (or 1,5- if 9,10-positions are blocked by sterically nonhindering substituents).
- [27] **1,5-A(5,6)** was not isolated and the isomeric ratio was deduced from ¹H NMR analysis of the crude reaction mixture.
- [28] C. Poriel, F. Barrière, D. Thirion, J. Rault-Berthelot, *Chem. Eur. J.* **2009**, *15*, 13304–13307.
- [29] A. Dadvand, W.-H. Sun, A. Moiseev, F. Bélanger-Gariépy, F. Rosei, H. Meng, D. F. Perepichka, *J. Mater. Chem. C* **2013**, *1*, 2817–2825.
- [30] S. Hamai, F. Hirayama, *J. Phys. Chem.* **1983**, *87*, 83–89.
- [31] P. Rapti, N. Schulte, A. D. Schlüter, L. Dunsch, *Chem. Eur. J.* **2006**, *12*, 3103–3113.
- [32] One could expect a larger relative stabilization of the SOMO due to solvation in the smaller BIN radical cation, which would decrease the HOMO–SOMO and increase the SOMO–LUMO transition energies (more so than for the larger BIA radical cation).
- [33] C. B. Nielsen, A. Angerhofer, K. A. Abboud, J. R. Reynolds, *J. Am. Chem. Soc.* **2008**, *130*, 9734–9746.
- [34] Gaussian 09, Revision B.01, M. J. Frisch, G. W. Trucks, H. B. Schlegel, G. E. Scuseria, M. A. Robb, J. R. Cheeseman, G. Scalmani, V. Barone, B. Mennucci, G. A. Petersson, H. Nakatsuji, M. Caricato, X. Li, H. P. Hratchian, A. F. Izmaylov, J. Bloino, G. Zheng, J. L. Sonnenberg, M. Hada, M. Ehara, K. Toyota, R. Fukuda, J. Hasegawa, M. Ishida, T. Nakajima, Y. Honda, O. Kitao, H. Nakai, T. Vreven, J. A. Montgomery, Jr., J. E. Peralta, F. Ogliaro, M. Bearpark, J. J. Heyd, E. Brothers, K. N. Kudin, V. N. Staroverov, R. Kobayashi, J. Normand, K. Raghavachari, A. Rendell, J. C. Burant, S. S. Iyengar, J. Tomasi, M. Cossi, N. Rega, J. M. Millam, M. Klene, J. E. Knox, J. B. Cross, V. Bakken, C. Adamo, J. Jaramillo, R. Gomperts, R. E. Stratmann, O. Yazyev, A. J. Austin, R. Cammi, C. Pomelli, J. W. Ochterski, R. L. Martin, K. Morokuma, V. G. Zakrzewski, G. A. Voth, P. Salvador, J. J. Dannenberg, S. Dapprich, A. D. Daniels, O. Farkas, J. B. Foresman, J. V. Ortiz, J. Cioslowski, D. J. Fox, Gaussian, Inc., Wallingford CT, **2009**.

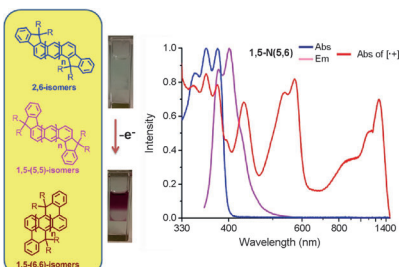
Received: December 26, 2014

Published online on ■■■, 0000

FULL PAPER

Indenofluorenes

M. R. Rao, A. Desmecht, D. F. Perepichka*

**π-Extended Indenofluorenes**

An extended family: A series of aromatic indenofluorene (IF) analogues with naphthalene and anthracene cores have been synthesized (see figure; **1,5-N(5,6)** is an isomer of a naphthalene derivative). Compared with the parent IF, the extended acene core endows red-shifted absorption and emission spectra and lowered oxidation potentials.